



Dermal exposure to particle-bound polycyclic aromatic hydrocarbons from barbecue fume as impacted by physicochemical conditions[☆]

Jia-Yong Lao^a, Si-Qi Wang^a, Yun-Qi Chen^a, Lian-Jun Bao^a, Paul K.S. Lam^b,
Eddy Y. Zeng^{a,*}

^a Guangdong Key Laboratory of Environmental Pollution and Health, School of Environment, Jinan University, Guangzhou, 511443, China

^b State Key Laboratory of Marine Pollution, Department of Chemistry, City University of Hong Kong, Hong Kong, China

ARTICLE INFO

Article history:

Received 8 November 2019

Received in revised form

23 January 2020

Accepted 24 January 2020

Available online 30 January 2020

Keywords:

Particle-bound polycyclic aromatic hydrocarbons
Barbecue fume
Dermal exposure
Forearms wipe
Gas-particle distribution

ABSTRACT

Inhalation of size-dependent particle-bound polycyclic aromatic hydrocarbons (PAHs) has been extensively studied, whereas dermal absorption has not been adequately investigated. To address this knowledge gap, dermal absorption of size-dependent particle-bound PAHs was characterized through the collection of indoor air and forearm wipe samples in the setting of an indoor barbecue. The mass of size-fractionated PAHs associated with particulate matter was greater in fine particles (<1.8 μm) than in coarse particles (>1.8 μm). Gas-particle distribution of specific PAHs from barbecue fume was ascribed to both adsorption and absorption which would probably be close to equilibrium, while that from background air was dominated by absorption. Forearm-deposited amounts of particulate PAHs suggested that removal of coarse and fine particles could minimize exposure to low and high molecular-weight (MW) PAHs, respectively. Besides, the concentrations of particulate PAHs in forearms wipe were significantly correlated to their dry deposition fluxes with coarse particles, but weakly correlated to those with fine particles. This indicated that particle size would influence dermal absorption efficiency of particle-bound PAHs with fine particles prolonging dermal exposure to PAHs. Overall, higher MW particle-bound PAHs derived from barbecue fume may pose higher risk to human health by dermal absorption than lower MW PAHs.

© 2020 Elsevier Ltd. All rights reserved.

1. Introduction

Numerous studies have focused on inhalation of particulate matter (PM), especially fine PM, since they can penetrate deep into the lung and even into the blood stream, causing respiratory and cardiovascular disease and cancer (Mills et al., 2008; Sun et al., 2005; WHO, 2019). Aside from the concern on inhalation of PM, dermal absorption of PM also deserves attention. Exposure to PM could induce oxidative stress and skin aging, as well as negatively affect fundamental skin functions (Dick et al., 2003; Kim et al., 2016; Verdin et al., 2019; Vierkoetter et al., 2010). Hirai et al. (2012) suggested that nanoparticles could enter epidermal Langerhans cells, dermis cells, and regional lymph nodes in mice. Nanoparticles could also penetrate deep into the skin layer via hair follicles, resulting in greater dermal absorption (Adib et al., 2016;

Frombach et al., 2019; Lademann et al., 2004). It is worthwhile to note that absorption of PM by skin is size-dependent (Adib et al., 2016; Kim et al., 2016; Lademann et al., 2004), which thus must be considered in any risk assessment.

Because PM is a strong sorption matrix for organic chemicals, organic contaminants associated with PM are of ultimate importance for health risk assessment. In this context, polycyclic aromatic hydrocarbons (PAHs) deserve particular attention due to their widespread occurrence and abundance in the environment, as well as their adverse threats to human health (WHO, 2019). In particular, high molecular-weight (HMW) PAHs (MW ≥ 228 g mol⁻¹) are mostly associated with particles, augmenting the significance for evaluating dermal absorption of particle-bound PAHs (Lao et al., 2018b; Luo et al., 2015; Shen et al., 2011). Among the various important sources of PAHs, barbecue (BBQ; grilling foods over hot charcoal) fume has been reported to generate abundant particle-bound PAHs (Badyda et al., 2017; Wu et al., 2015), which can provide a suitable experimental setting for a comprehensive investigation into the dermal absorption of particle-bound PAHs.

[☆] This paper has been recommended for acceptance by Christian Sonne.

* Corresponding author.

E-mail address: eddyzeng@jnu.edu.cn (E.Y. Zeng).

Size dependence, gas-particle distribution, and deposition flux have great influences on dermal absorption of particle-bound PAHs. Despite this, size dependence for dermal absorption of particle-bound PAHs has rarely been examined. Gas-particle distribution has a great impact on the atmospheric fate of a chemical (Lohmann and Lammel, 2004), whereas deposition flux dictates the removal of the chemical from the atmosphere (Tasdemir and Esen, 2007; Zhang et al., 2012). Gas-particle distribution and deposition flux combined may determine, to a large extent, the amount of particle-bound PAHs deposited on human body surfaces and eventually dermal absorption efficiency, but there remains a knowledge gap on how dermal exposure to particle-bound PAHs may be modulated by certain important physicochemical conditions. Although skin wipe is becoming a popular indicator of dermal exposure to pollutants and has been reported to be correlated with dust (Cao et al., 2019; Gong et al., 2014; Tan et al., 2018), dermal absorption of particle-bound PAHs by skin wipe has not been adequately studied. Modeling approaches, commonly used to evaluate dermal absorption, have also not been adequately used to examine dermal absorption of size-dependent particle-bound PAHs (Gungormus et al., 2014; Shi and Zhao, 2014), as they have been used to mainly investigate inhalation of size-dependent particle-bound PAHs instead of dermal absorption.

A comprehensive investigation of barbecue fume would shed light on the above-mentioned knowledge gap and may assist in identifying ways to minimize dermal absorption of particle-bound PAHs. An indoor barbecue event was held in Guangzhou, Guangdong Province of China and served as a case study. Indoor air samples of background (before barbecue) and barbecue fume (during barbecue), as well as forearm wipes from 12 male participants, were collected and analyzed for PAHs. The objectives were to (1) obtain the profiles of particle-bound PAHs and examine the possible mechanisms for association between PAHs and particles; (2) obtain the gas-particle distribution of PAHs derived from barbecue fume, and then identify their transport patterns; and (3) estimate dry deposition flux of particle-bound PAHs from barbecue fume and their dry deposited amounts on forearms, and combine the results of forearm wipes to characterize their dermal absorption in relation to particle size.

2. Materials and methods

2.1. Materials

Sixteen priority PAHs designated by the United States Environmental Protection Agency, including naphthalene (Nap), acenaphthylene (Acy), acenaphthene (Ace), fluorene (Flu), phenanthrene (Phe), anthracene (Ant), fluoranthene (Fla), pyrene (Pyr), benzo[*a*]anthracene (BaA), chrysene (Chr), benzo[*b*]fluoranthene (BbF), benzo[*k*]fluoranthene (BkF), benzo[*a*]pyrene (BaP), indeno[1,2,3-*cd*]pyrene (IcdP), dibenz[*ah*]anthracene (DahA), and benzo[*ghi*]perylene (BghiP), were supplied by AccuStandard (New Haven, CT). The sum of 16 PAHs is defined as $\sum_{16}\text{PAH}$. Naphthalene-*d*₈, acenaphthene-*d*₁₀, phenanthrene-*d*₁₀, chrysene-*d*₁₂, perylene-*d*₁₂, and benzo[*ghi*]perylene-*d*₁₂ employed as surrogate standards and 2-fluorobiphenyl, *p*-terphenyl-*d*₁₄, and dibenzo[*ah*]anthracene-*d*₁₄ employed as internal standards were purchased from Dr. Ehrenstorfer GmbH (Augsburg, Germany).

2.2. Sampling strategy

As indoor BBQ restaurants have become increasingly prevalent in recent years and meats grilled by charcoal for better flavor are much more preferable, indoor barbecue should draw a lot of attention from the public. Therefore, a new office room on the top

floor of a four-story building located in Guangzhou suburban areas was chosen to conduct an indoor barbecue event from 14:30 to 17:30 on January 6, 2018, with charcoal as the heating source and meat as the main food type (mostly pork, but also including chicken, beef, and fish meat balls). While foods were being grilled, the windows and door were open for ventilation. Detailed sampling information of the indoor barbecue event was presented in the supporting information of our previous publication (Lao et al., 2018c). Briefly, 12 adult males aged 22 to 29 were invited to wear the same types of T-shirts and shorts and participated in the sampling campaign. After 3-h exposure to barbecue fume, 7 cm × 7 cm precleaned gauze pads soaked with ethanol were applied to wipe the forearms of the participants (one piece of gauze pad for each forearm), which were then stored in polytetrafluoroethylene tubes containing 30 mL of dichloromethane.

A Micro-Orifice Uniform Deposit Impactor (MOUDI) (MSP Corporation, Shoreview, MN) equipped with 47-mm diameter glass microfiber filters (Whatman International, Maidstone, England), end-connected to polyurethane foam, was applied to collect particle and gaseous samples at a constant flow rate of 30 L min⁻¹. Each particle sample was segregated into 11 size fractions: >18, 10–18, 5.6–10, 3.2–5.6, 1.8–3.2, 1.0–1.8, 0.56–1.0, 0.32–0.56, 0.18–0.32, 0.10–0.18, and 0.056–0.10 μm. Indoor air samples of barbecue fume were collected for 3 h at two sites (Fig. S1; Sites 1 and 2 were near the door and windows, respectively). Additionally, air samples of indoor background were collected for 29 h from 12:30 on January 4 to 17:30 on January 5. Overall, 33 size-fractioned particle, three gaseous, and 12 forearm wipe samples, as well as related field blank samples, were obtained. All these samples were stored at -20 °C and analyzed as soon as possible.

2.3. Sample extraction and instrumental analysis

Procedures of sample extraction and purification were described in detail previously (Lao et al., 2018c), and only a brief description is given herein. Prior to extraction, all the samples were spiked with surrogate standards. Particulate and gaseous samples were extracted by sonication and Soxhlet extraction, respectively, with a mixture of hexane, dichloromethane, and acetone (2:2:1 in volume). Forearm wipe samples were sonicated three times with 30 mL of dichloromethane for 30 min. Each extract was concentrated, solvent-exchanged to hexane, and further concentrated to 1 mL with a Zymark TurboVap 500 (Hopkinton, MA). The concentrated extract was dried with anhydrous sodium sulfate and purified on a neutral silica gel column with 20 mL of hexane as the eluent. The collected extract was further concentrated to 50 μL in a vial under a gentle stream of nitrogen and spiked with the internal standards before instrumental analysis.

All extracts were analyzed with a Shimadzu GCMS-2010 Plus in the electron impact mode. A DB-5MS capillary column (30 m × 0.25 mm i.d. with 0.25 μm film thickness) was used for chromatographic separation. Detailed information about column oven temperature program and other parameters was provided in a previous study (Lao et al., 2018b).

2.4. Quality assurance and quality control

The recoveries of the surrogate standards, i.e., naphthalene-*d*₈, acenaphthene-*d*₁₀, phenanthrene-*d*₁₀, chrysene-*d*₁₂, perylene-*d*₁₂, and benzo[*ghi*]perylene-*d*₁₂, were 70 ± 7%, 75 ± 7%, 74 ± 6%, 84 ± 10%, 78 ± 13%, and 83 ± 9% in blank samples and mean recoveries ranged from 69% to 87% in filed samples, presented in the supporting information of a previous study (Lao et al., 2018c). Concentrations of PAHs in field samples were corrected by those detected in the corresponding procedural blanks within the same

batch, but not corrected for the surrogate standard recoveries. The lowest calibration concentrations divided by the actual sample volumes/areas were defined as the reporting limits. The reporting limit was 0.005 ng m^{-3} with an air volume of 52.2 m^3 for gaseous and particulate samples from indoor background, 0.046 ng m^{-3} with an air volume of 5.4 m^3 for gaseous and particulate samples from barbecue fume, and 2.4 ng m^{-2} with an average forearm surface area of 0.104 m^2 for forearm wipe samples. Analyte concentrations below the reporting limits were set as zero in estimating deposition fluxes.

2.5. Data analysis

Gas-particle distribution coefficient (K_p ; $\text{m}^3 \mu\text{g}^{-1}$) of PAH was calculated with PAH concentrations in the particle (C_p ; ng m^{-3}) and gas phases (C_g , ng m^{-3}), and particulate matter concentration (C_{PM} ; $\mu\text{g m}^{-3}$) as below (Pankow, 1987, 1991).

$$K_p = \frac{C_p}{C_g \times C_{PM}} \quad (1)$$

The logarithm of subcooled liquid-vapor pressure ($\log P_L^0$; log (Pa)) was introduced to further understand the mechanism of gas-particle distribution. The relationship between $\log K_p$ and $\log P_L^0$ was described as (Pankow, 1994)

$$\log K_p = S_p \log P_L^0 + b_p \quad (2)$$

where S_p and b_p are constants, representing the slope and intercept, respectively. The octanol-air partition coefficients (K_{OA}) and P_L^0 at the measured temperature were calculated with the equations of Odabasi et al. (2006) and the data from the Estimation Programs Interface (EPI) Suite TM.

Dry deposition flux (F ; $\text{ng m}^{-2} \text{ h}^{-1}$) of PAH was estimated based on PAH concentration (C_{pi}) and particle dry deposition velocity (V_i) of each size fraction:

$$F = \sum (C_{pi} \times V_i) \quad (3)$$

where V_i was obtained from our previous study (Table S1) (Zhang et al., 2012). As our previous and the present studies used the same air sampler with the same particle size fractions, which is critical to estimate particle dry deposition velocities, and also collected air samples in Guangzhou during winter season (no significant difference of meteorological parameters between them). Hence, it is acceptable to use V_i estimated by Zhang et al. (2012).

Therefore, the amount of dry-deposited PAH on forearms (D_F ; ng) was estimated by

$$D_F = F \times SA \times f \times t \quad (4)$$

where SA is the body surface area of each participant (m^2), evaluated by Stevenson formula (Stevenson, 1937); f is the fraction of forearms to body surface area, and 6% was chosen (Boniol et al., 2008; Yu et al., 2010); and t is exposure time (h). As the concentrations of PAHs in forearm wipe and dry-deposited amounts of PAHs on forearm were calculated from the forearm surface area of each participant (Table S2), the correlation between the concentrations of PAHs in forearm wipes and dry deposition fluxes is the same as the correlation between the measured amounts of PAHs in forearm wipes and calculated dry-deposited amounts of PAHs on forearms. In the present study the first correlation will be further discussed.

Uncertainty and variability of the deposited amounts of PAHs on forearms were evaluated by Monte Carlo simulation. Significance

analysis was conducted with SPSS 20.0. Coarse and fine particles are defined as particle aerodynamic diameter >1.8 and $<1.8 \mu\text{m}$, respectively. Low and medium molecular-weights are denoted as LMW ($\text{MW} \leq 178 \text{ g mol}^{-1}$) and MMW ($178\text{--}228 \text{ g mol}^{-1}$), respectively (Table S3).

3. Results and discussion

3.1. Occurrence of particulate matter and PAHs in ambient air

The PM contents were $90.6 \mu\text{g m}^{-3}$ in background air, and 3280 and $3760 \mu\text{g m}^{-3}$ in barbecue fume at two sampling sites (Table 1). The mass fraction of coarse particles (59%) dominated total PM in background air (Fig. 1a). Particles in the size range of $0.56\text{--}5.6 \mu\text{m}$ have lower deposition velocities than other sized particles (Table S1) (Zhang et al., 2012; Zhang et al., 2001). As a result, they dominated total PM in indoor air as they were subject to less losses going from outdoor to indoor sources. By contrast, the mass fraction of coarse particles ($47.9 \pm 1.3\%$) in barbecue fume was smaller than that of fine particles ($52.2 \pm 1.3\%$). The mass fraction ($39.7 \pm 1.2\%$) of particles with sizes greater than $18 \mu\text{m}$ contributed the most to the mass of PM compared to other size fractions (Fig. 1a). Therefore, PM from barbecue fume followed a bimodal distribution pattern, peaking in the fine ($<1.8 \mu\text{m}$) and coarse ($>18 \mu\text{m}$) fractions. Badyda et al. (2017) showed that combustion of lump charcoal without food loaded contributed greater PM contents in coarse particles than in fine particles. After food was loaded, however, contents of fine particles increased rapidly (Badyda et al., 2017). Badyda et al. (2017) further pointed out that almost no coarse particles were produced by liquid propane gas combustion, which also could eliminate soot formation. As coarse particles are largely generated by mechanical processes, as in the present study, formation of coarse particles is mostly attributed to charcoal combustion, whereas food plays an irreplaceable and important role in fine particle formation (Wilson and Suh, 2012).

Gaseous BbF, BkF, BaP, IcdP, DahA, and BghiP ($\text{MW} \geq 252 \text{ g mol}^{-1}$) with low vapor pressures were not detected in indoor background air and barbecue fume. In addition, concentrations of particle-bound DahA were also below the reporting limit in background air (Table S4). Overall, gaseous PAH concentrations in background air and barbecue fume at sites 1 and 2 were 37 , 770 , and 1127 ng m^{-3} , respectively, whereas particulate PAH concentrations were 4.2 , 595 , and 629 ng m^{-3} , respectively (Table 1). Apparently, indoor barbecue contributed great amounts of PAHs in ambient air. The current indoor barbecue generated lower concentrations of gaseous PAHs but higher concentrations of particle-bound PAHs than those in Urumqi and Guangzhou suburban area (2900 ± 480 and 1160 ng m^{-3} , respectively, for gaseous PAHs; and 320 ± 265 and 52 ng m^{-3} , respectively, for particle-bound PAHs) (Wu et al., 2015). However, it should be noted that only one barbecue stove was employed to conduct this event, while several barbecue sites or stoves were combined to carry out the previous studies.

There is a natural inclination for PAHs to shift from the gas phase to the particle phase with increasing benzene rings (Table 1), largely due to lower vapor pressures for higher MW PAHs. For barbecue fume, PAHs with MW higher than 202 g mol^{-1} (≥ 3 rings) were mostly associated with particles. Background PAHs of indoor air with MW higher than 252 g mol^{-1} (≥ 5 rings) existed almost entirely in the particle phase (Tables 1 and S3). By comparison, barbecue fume generated a wider range of PAHs predominantly associated with the particle phase. This was probably because PAHs generated from barbecue fume were freshly formed with high abundances and emitted to gas phase at higher temperatures of grilling, and thus were readily associated with particles by

Table 1
Concentrations of airborne polycyclic aromatic hydrocarbons (PAHs) (C_p and C_g for particle and gas phases respectively; ng m^{-3}) and particulate matter (PM; $\mu\text{g m}^{-3}$) during indoor barbecue sampling period.

	2 rings ^a		3 rings		4 rings		5-6 rings		$\sum_{16}\text{PAH}_p^b$	$\sum_{16}\text{PAH}_g^c$	PM
	C_p	C_g	C_p	C_g	C_p	C_g	C_p	C_g			
Background	0.34	16.6	0.52	17.6	1.68	2.64	1.66	<RL ^d	4.20	37	90.6
Site 1	18.6	567	223	183	264	19.1	89.8	<RL ^e	595	770	3280
Site 2	11.0	758	253	334	271	35.9	94.1	<RL ^f	629	1127	3760

^a 2 rings: the sum of PAH with two aromatic rings.

^b $\sum_{16}\text{PAH}_p$: concentrations of particulate 16 priority PAHs.

^c $\sum_{16}\text{PAH}_g$: concentrations of gaseous 16 priority PAHs.

^d RL: the acronym of the reporting limit at 0.005 ng m^{-3} with an air volume of 52.2 m^3 .

^e RL: the acronym of the reporting limit at 0.046 ng m^{-3} with an air volume of 5.4 m^3 .

^f RL: the acronym of the reporting limit at 0.046 ng m^{-3} with an air volume of 5.4 m^3 .

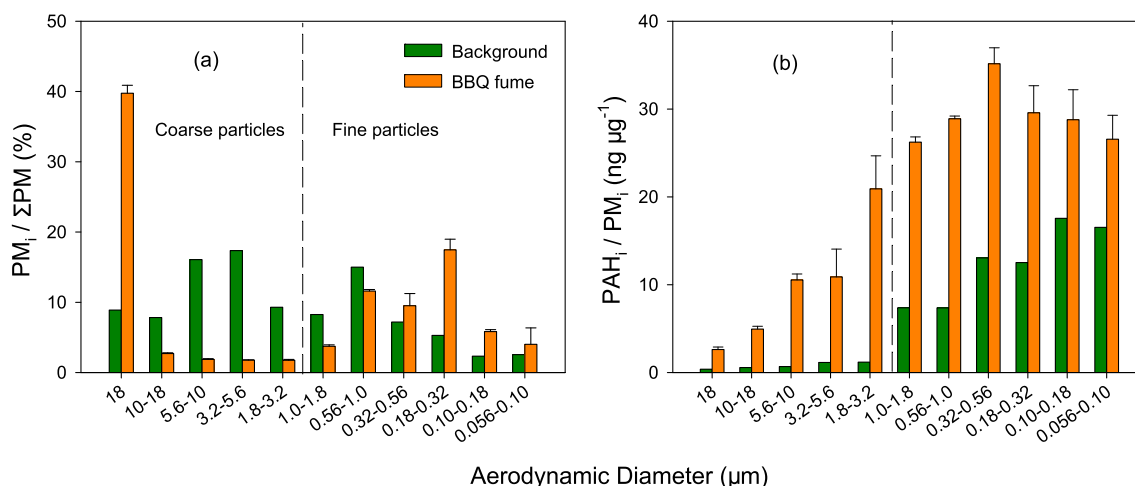


Fig. 1. The mass fractions of (a) each size-fractionated particulate matter (PM_i) to total particles (ΣPM) and (b) each size-fractionated particle-bound PAHs (PAH_i) to related fractionated particulate matter for background level and barbecue fume, where i represents the size fraction of aerodynamic diameter.

nucleation or coagulation/condensation (Wilson and Suh, 2012). In addition, outdoor atmospheric PAHs may have undergone transport and transformation and partially deposited to the ground before diffusing to indoor environments, resulting in a narrower range of molecular weights for PAHs associated with background air particles.

The mass fractions of size-fractionated particulate PAHs associated with PM showed similar distribution patterns in background air and barbecue fume. Specifically, the mass fractions in fine particles were greater than those of coarse particles (Fig. 1b), i.e., fine particles possessed greater capacity of accumulating PAHs. Many studies demonstrated that particle number concentration is often greater in fine sizes than in coarse sizes, which also possess much more particle surface areas (Harrison et al., 2000; Hu et al., 2018; Vallero, 2014). These attributes allow fine particles to accumulate abundant PAHs by adsorption and absorption. This also explains why barbecue fume contained abundant PAHs in fine particles.

3.2. Gas-particle distribution

The distribution of PAHs between the gas and particle phases somewhat dictates the fate and potential human health risk of PAHs. Gas-particle distribution of PAHs may be influenced by the physicochemical properties of both PAHs and aerosols as well as meteorological conditions, e.g., vapor pressures of PAHs, compositions and surface areas of aerosols, and temperature, etc. (Sitaras et al., 2004; Wu et al., 2014). In the present study, 10 PAHs, detected in the gas phase, were used to estimate gas-particle distribution

coefficient (K_p). The $\log K_p$ for these 10 PAHs in background air and barbecue fume were in the ranges of -2.01 – (-4.10) and -2.13 – (-6.25) , respectively, and higher MW PAHs showed stronger tendency to adhere to particles (Table S5). The $\log K_p$ values of PAHs with $MW \geq 178 \text{ g mol}^{-1}$ (≥ 3 rings) were quite similar in background air and barbecue fume, whereas those of PAHs with $MW \leq 166 \text{ g mol}^{-1}$ (≤ 2 rings) varied widely (Table S5). This large variability may be attributed to the high vapor pressures of LMW PAHs which are more affected by varying temperatures and emission sources compared to HMW PAHs.

Because physical adsorption and absorption occur on the surfaces of aerosols and into aerosol organic matter, respectively (Dachs and Eisenreich, 2000; Pankow, 1994), the $\log K_p$ – $\log P_p^0$ model is used to determine if gas-particle distribution is related predominantly to adsorption or absorption (Goss and Schwarzenbach, 1998). Equation (2) suggests that gas-particle distribution is dominated by absorption when $S_p \geq -0.6$ and by adsorption when $S_p \leq -1$. Values of S_p between -1 and -0.6 indicate both adsorption and absorption are equally important (Goss and Schwarzenbach, 1998; Pankow, 1994). In the present study, a better linear correlation between $\log K_p$ and $\log P_p^0$ of PAHs was found for barbecue fume ($r^2 = 0.96$) than for background air ($r^2 = 0.67$) (Fig. 2a and b). The slope of the linear regression equation for background PAHs in ambient air was -0.31 , suggesting absorption as the predominant mechanism for gas-particle distribution of PAHs. The slope was -0.75 for barbecue fume, i.e., both adsorption and absorption were equally important. Moreover, the octanol-air partition coefficient (K_{OA}) is a direct descriptor of gas-

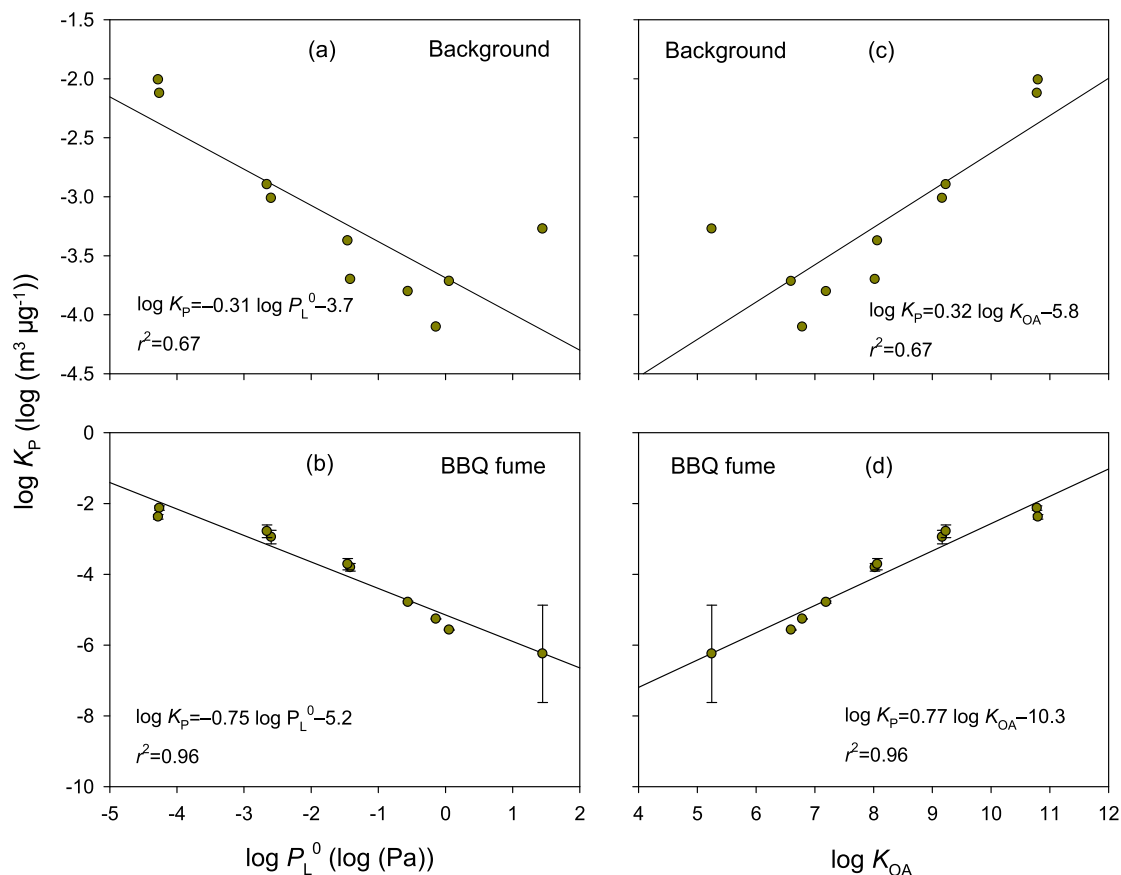


Fig. 2. Correlations of the logarithms of PAH gas-particle distribution coefficients ($\log K_p$) with (a, b) the logarithms of subcooled liquid-vapor pressures ($\log P_L^0$), and (c, d) the logarithms of octanol-air partition coefficients ($\log K_{OA}$).

particle distribution for semi-volatile organic chemicals, dominated by absorption (Finizio et al., 1997). The $\log K_p$ of PAHs was positively correlated to $\log K_{OA}$ for both background air ($r^2 = 0.67$) and barbecue fume ($r^2 = 0.96$) (Fig. 2c and d). As adsorption and absorption are strongly dependent on elemental carbon (e.g., soot) and organic matter, respectively, in aerosols (Yu and Yu, 2012), measurement of both constituents is conducive for further examining gas-particle distribution.

For $\log K_p$ – $\log K_{OA}$ model, the slope close to 1 means equilibrium partitioning of absorption (Lohmann et al., 2000). Hence, our results suggest that gaseous PAHs generated by barbecue fume approached to equilibrium absorption with particles (Liu et al., 2015), whereas background PAHs in ambient air remained in non-equilibrium state of absorption. For $\log K_p$ – $\log P_L^0$ model, the equilibrium state is also characterized by a slope value close to -1 . A deviation from -1 , however, does not necessarily mean non-equilibrium for adsorption and absorption, suggested by Goss and Schwarzenbach (1998). Besides, based on the model estimation, PAHs with $MW \leq 202 \text{ g mol}^{-1}$ can almost reach equilibrium in all particle size fractions within 1 h for adsorption and absorption, while it would take HMW PAHs longer time to achieve equilibrium (Yu and Yu, 2012). It was possible that both adsorption and absorption of 10 PAHs derived from barbecue fume approached to equilibrium.

Temperature is another significant parameter that can greatly influence desorption and volatilization of particle-bound PAHs. Gaga and Ari (2011) suggested that more sorbed PAHs tend to escape from particles to the gas phase as temperature increases. As

human body surface might have higher temperatures than the measured temperature of ambient air in the present study (16°C), particle-bound PAHs deposited on human body surface possibly tend to migrate to the gas phase, contributing to higher concentrations of gaseous PAHs above the skin surface. In particular, concentrations of gaseous LMW PAHs around the body surface may have been underestimated, as lower K_p indicated greater capability for LMW PAHs to escape from the particle phase.

3.3. Dry deposition flux and deposited amount on forearms

Because particle-bound PAHs are dependent on particle size, it is crucial to choose size-fractionated dry deposition velocities for estimating dry deposition fluxes. The size-fractionated dry deposition velocities calculated by Zhang et al. (2012) were adopted in the present study. Fine particles contributed to $\sum_{16}\text{PAH}$ more than coarse particles in both background air and barbecue fume (Table S6). This pattern seems to vary with different studies (Kaupp and McLachlan, 1999; Lin et al., 1994; Zhang et al., 2012), due to strong effects of emission sources and meteorological conditions. Dry deposition fluxes of most individual PAHs, except for Ace and Flu, were predominated by fine particles in background air (Fig. 3a). For barbecue fume, fine particles increasingly predominated dry deposition fluxes of PAHs with increasing MW, except for Nap (Fig. 3b and c). Dominance of the dry deposition fluxes of LMW PAHs by coarse particles was largely attributed to high dry deposition velocities of coarse particles.

From dry deposition flux and exposed surface area and time, the

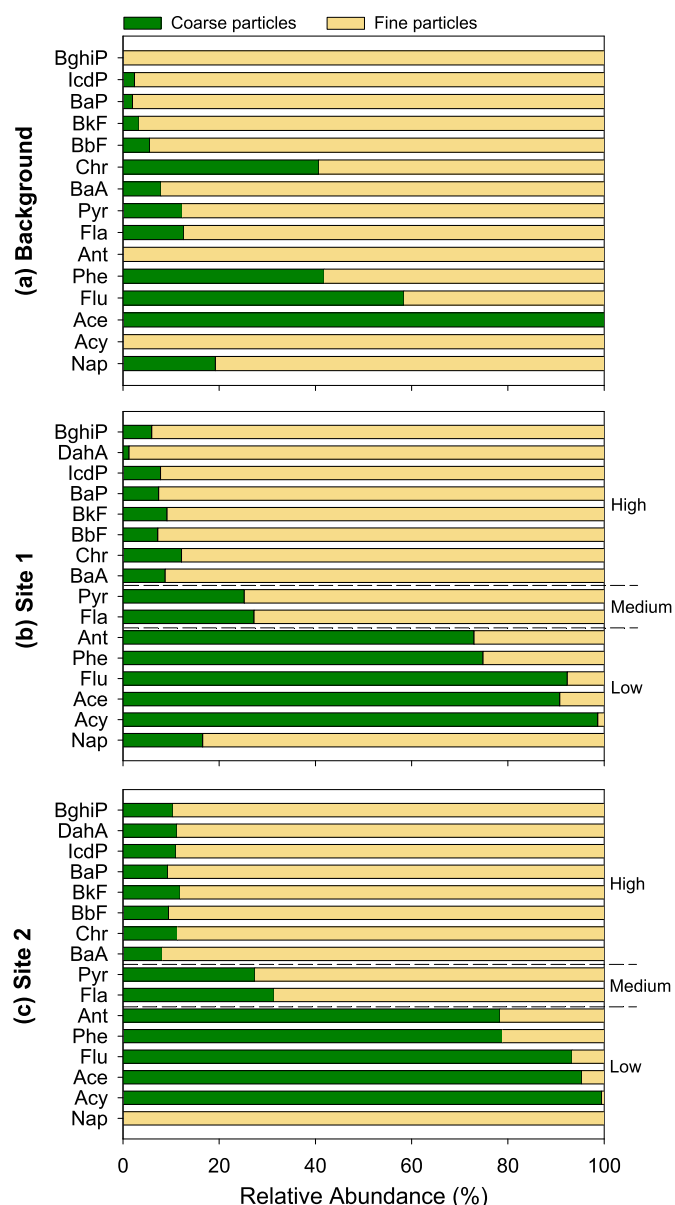


Fig. 3. Calculated relative abundance (%) of dry deposition fluxes of particle-bound PAHs by coarse and fine particles on (a) background site and (b, c) two barbecue sampling sites. “Low”, “Medium”, and “High” represents low, medium, and high molecular-weight PAHs, respectively.

amounts of particle-bound PAHs deposited on forearms were estimated to be 820 ± 110 , 980 ± 72 , and 1800 ± 160 ng, respectively, by coarse particles, fine particles, and total particles from barbecue fume (Table 2). The majority of particulate LMW PAHs (except for Nap) on forearms surface was contributed by coarse particles, whereas the deposited amounts of MMW and HMW PAHs were mostly derived from fine particles. Skin penetration and retention of chemicals were also reported to depend upon particle size (Kim et al., 2016; Liu et al., 2018). Particles with aerodynamic dimeters $>1 \mu\text{m}$ can hardly penetrate into skin and therefore mostly deposit on skin surface, whereas fine particles may penetrate into skin through hair follicles (Kim et al., 2016; Lademann et al., 2004). Lademann et al. (2007) demonstrated that nanoparticles were able to store up to 10 days in hair follicles. Hair follicles could break the barrier built by stratum corneum and facilitate dermal absorption through follicular penetration (Kim

Table 2
Dry deposition amounts (ng) of particle-bound polycyclic aromatic hydrocarbons (PAHs) on forearms and total amounts (ng) of PAHs on forearms wipe after 3-h exposure to indoor barbecue fume.

	Deposited amount on forearms			Forearms wipe
	Coarse particles	Fine particles	Total particles	
Nap	2.04 ± 2.05^a	10.3 ± 10.3	12.4 ± 12.3	2.23 ± 0.58
Acy	39.9 ± 11.6	0.33 ± 0.06	40.3 ± 11.5	5.58 ± 3.97
Ace	6.78 ± 1.84	0.46 ± 0.05	7.25 ± 1.81	1.48 ± 1.03
Flu	67.1 ± 13.2	5.09 ± 0.66	72.2 ± 13.9	12.3 ± 4.6
Phe	427 ± 92	126 ± 14	554 ± 106	84.3 ± 29.0
Ant	88.6 ± 19.3	27.8 ± 2.5	116 ± 22	15.6 ± 6.3
Fla	72.0 ± 14.8	171 ± 20	243 ± 34	16.0 ± 3.9
Pyr	65.6 ± 11.4	182 ± 22	248 ± 34	13.5 ± 3.4
BaA	6.90 ± 0.62	74.6 ± 8.9	81.5 ± 9.5	4.55 ± 2.07
Chr	13.8 ± 1.2	104 ± 12	118 ± 13	3.31 ± 1.08
BbF	7.45 ± 1.92	80.3 ± 10.1	87.8 ± 12.0	4.49 ± 1.81
BkF	2.42 ± 0.73	20.1 ± 3.4	22.5 ± 4.1	5.65 ± 3.16
BaP	5.09 ± 1.25	55.0 ± 7.4	60.1 ± 8.6	<RL ^b
IcdP	3.85 ± 1.26	36.0 ± 5.7	39.8 ± 6.9	<RL
DahA	1.07 ± 0.92	13.9 ± 2.1	15.0 ± 2.9	<RL
BghiP	6.76 ± 2.95	72.0 ± 12.2	78.8 ± 15.2	<RL
$\Sigma_{16}\text{PAH}$	817 ± 107	979 ± 72	1800 ± 160	169 ± 53

^a Data are presented as mean \pm standard deviation.

^b RL: the acronym of the reporting limit at 0.25 ng.

et al., 2016). Because MMW and HMW PAHs are mostly associated with fine particles, they can be more readily absorbed and thus pose a potentially higher risk to human health. If fine particles on skin cannot be removed effectively, their adverse impacts may persist. Conversely, removal of coarse particles after exposure is an effective way to minimize dermal absorption of LMW PAHs.

3.4. Forearm wipe—indication of coarse particles deposition

Skin wipe has been commonly used to evaluate human exposure to contaminants by dermal absorption or dust-to-mouth contact (Poothong et al., 2019; Stapleton et al., 2008; Tan et al., 2018). Forearm wipe was employed in the present study to examine particle deposition on human skin and the underlying mechanism of dermal absorption, which was deemed feasible as particles depositing on forearms cannot be easily removed by participants’ movement during the barbecue event. After 3-h exposure to barbecue fume, some individual PAHs on forearms were detected, with concentrations ranging from 1.48 ± 1.03 to 84.3 ± 29.0 ng (Table 2), the concentrations of Bap, IcdP, DahA, and BghiP (≥ 5 rings) remained below the reporting limits. As mentioned above, HMW PAHs are mostly adhered to fine particles, which can be trapped in hair follicles so that they are more readily absorbed and are not easily wiped off (Beaucham et al., 2019). In addition, fine particles depositing on skin may release HMW PAHs, with dermal absorption enhanced by increasing temperature. The transdermal permeability coefficients of HMW PAHs are also remarkably greater than those of LMW PAHs (Lao et al., 2018). All these may have been the reasons why Bap, IcdP, DahA, and BghiP were not detected on forearm wipes. The difference between the amounts of particle-bound PAHs on forearms and forearm wipes suggested efficient absorption of PAHs by forearm skin surface and/or reactions of PAHs on skin surface, but more evidence is needed to verify such hypothesis.

Concentrations of individual PAHs on forearm wipe were normalized by the surface area of each participant’s forearms (Fig. 4). Concentrations of PAHs on forearm wipe and dry deposition fluxes of total particle-bound PAHs were significantly correlated ($r^2 = 0.85$; $p < 0.01$; Fig. 5). Furthermore, PAH concentrations on forearm wipe were strongly correlated with dry deposition fluxes

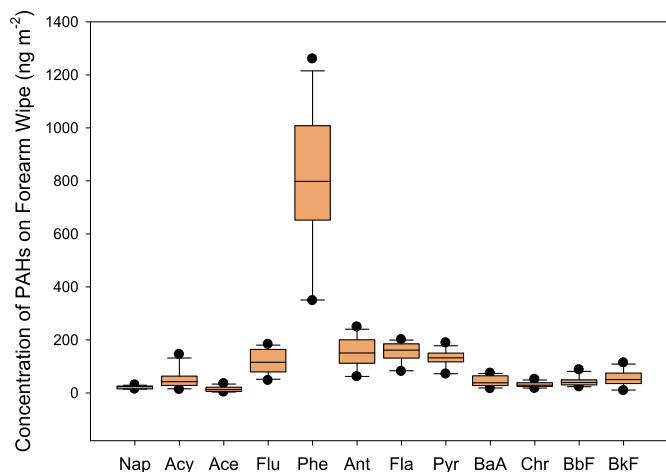


Fig. 4. Concentrations (ng m^{-2}) of PAH on forearms wipe of 12 participants after exposure to 3 h barbecue fume.

of coarse particles ($r^2 = 0.99$; $p < 0.01$), but only weakly correlated with those of fine particles ($r^2 = 0.14$; $p > 0.05$) (Fig. 5). This was in accordance with a previous finding that coarse particles mostly deposited on skin surface (Lademann et al., 2004). It also suggested that fine particles could be more easily absorbed, explaining why HMW PAHs were hardly detected on forearm wipe.

Because of the strong correlation between PAH concentrations in forearm wipe and coarse particles (Fig. 5b), bathing may be able to effectively remove coarse particle-bound PAHs after exposure to barbecue fume (Watkins et al., 2011). Suitable clothes may also play an important role in minimizing the deposition of coarse particles on skin surface. However, it may be more difficult to remove fine particles as hand-wash with soap and water is not effective enough (Esswein et al., 2011). Overall, HMW particle-bound PAHs have higher negative impacts on human health than LMW ones, partially attributed to particle size effects.

3.5. Implications and limitations

High MW PAHs derived from BBQ fume are more readily associated with fine particles (Table S4), which tended to deposit on surfaces of human body. Hair follicles account for about 10% of the surface area of scalp and face, and serve as a large reservoir for fine particles (Kim et al., 2016). These body parts as well as forearms are readily exposed to particles, posing a high potential risk to human health through dermal absorption of particle-bound PAHs. Forearm wipe results indicated that fine particles were more difficult to be effectively removed than coarse particles. They were probably trapped in hair follicles, potentially leading to prolonged exposure. Wearing suitable clothes during exposure or effectively washing these body parts after exposure to barbecue fume may reduce the amounts of particle-bound PAHs by dermal absorption.

Size-dependent dermal absorption of particle-bound PAHs has been carefully examined in the present study, but more works are still needed. One example is to determine the effects of physiological factors on dermal absorption efficiency of size-dependent particle-bound PAHs. To accomplish this goal, blood samples of the exposed individuals should be included to complement ambient air samples. As stratum corneum acts as skin barrier and its thickness varies with different body parts, it may be instructive to examine the effects of stratum corneum thickness on dermal absorption of particle-bound PAHs. Lipid may accelerate dermal absorption of PAHs by intercellular routes, thus measurement of

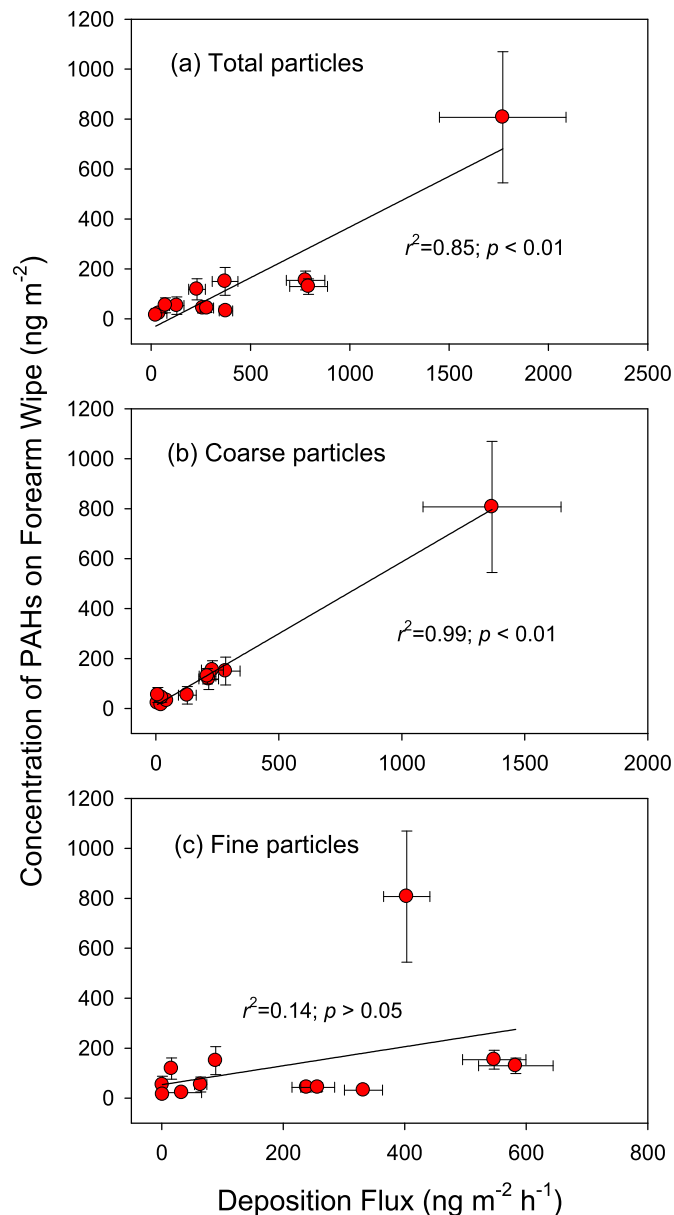


Fig. 5. Correlations of PAH concentrations (ng m^{-2}) on forearms wipe with barbecue fume dry deposition fluxes ($\text{ng m}^{-2} \text{h}^{-1}$) of (a) total particles, (b) coarse particles, and (c) fine particles.

lipid on skin surface could help understand the efficiency of dermal absorption. Finally, to better estimate indoor dry deposition fluxes of particle-bound PAHs and deposited amounts on forearms, meteorological conditions at a specific site should be acquired and used to refine the calculation of dry deposition velocities.

4. Conclusions

Barbecue by charcoal generated a great amount of particulate matter, which was dominated by size fractions of <1.8 and $>18 \mu\text{m}$, probably resulted from food grilling and charcoal combustion, respectively. Higher MW particle-bound PAHs derived from barbecue fume showed stronger tendency to adhere to particles and could approach to equilibrium between the gas and particle phases, ascribed to both adsorption and absorption. Dry deposition of coarse and fine particles dominated forearm-deposited amounts

of low and high MW PAHs, respectively. Moreover, particle-bound PAHs in coarse particles could be more readily to be wiped off than those in fine particles. All these indicated that higher MW PAHs in fine particles may prolong their dermal exposure and pose potential risk by dermal absorption.

Author statement

The authors declare that there is no competing interest among all authors.

Declaration of competing interest

The authors declare that the research was conducted in the absence of any commercial or financial relationships that could be construed as a potential conflict of interest.

Acknowledgments

Financial support of the present study from the National Natural Science Foundation of China (Nos. 21637001 and 21722701) was gratefully acknowledged. Special thanks go to Shan-Yi Xie, Ting-Yu Li, Yuan-Jie Hu, Ying Dong, and Zi-Min Yu for collection of indoor air and forearm wipe samples, to Xia-Wen Qiu, Jia-Li Ge, and Chen Xie for experimental assistance, and to all participants for kindly offering forearm wipe samples.

Appendix A. Supplementary data

Supplementary data to this article can be found online at <https://doi.org/10.1016/j.envpol.2020.114080>.

References

Adib, Z.M., Ghanbarzadeh, S., Kouhsoltani, M., Khosroshahi, A.Y., Hamishehkar, H., 2016. The effect of particle size on the deposition of solid lipid nanoparticles in different skin layers: A histological study. *Adv. Pharmaceut. Bull.* 6, 31–36.

Badyda, A.J., Widziejewicz, K., Rogula-Kozłowska, W., Majewski, G., Jureczko, I., 2017. Inhalation exposure to PM-bound polycyclic aromatic hydrocarbons released from barbecue grills powered by gas, lump charcoal, and charcoal briquettes. *Adv. Exp. Med. Biol.* 1023, 11–27.

Beaucham, C.C., Ceballos, D., Mueller, C., Page, E., La Guardia, M.J., 2019. Field evaluation of sequential hand wipes for flame retardant exposure in an electronics recycling facility. *Chemosphere* 219, 472–481.

Boniol, M., Verriest, J.P., Pedeux, R., Dore, J.F., 2008. Proportion of skin surface area of children and young adults from 2 to 18 years old. *J. Invest. Dermatol.* 128, 461–464.

Cao, Z.G., Zhao, L.C., Zhang, Y.C., Ren, M.H., Zhang, Y.J., Liu, X.T., Jie, J.Y., Wang, Z.Y., Li, C.H., Shen, M.H., Bu, Q.W., 2019. Influence of air pollution on inhalation and dermal exposure of human to organophosphate flame retardants: A case study during a prolonged haze episode. *Environ. Sci. Technol.* 53, 3880–3887.

Dachs, J., Eisenreich, S.J., 2000. Adsorption onto aerosol soot carbon dominates gas-particle partitioning of polycyclic aromatic hydrocarbons. *Environ. Sci. Technol.* 34, 3690–3697.

Dick, C.A.J., Brown, D.M., Donaldson, K., Stone, V., 2003. The role of free radicals in the toxic and inflammatory effects of four different ultrafine particle types. *Inhal. Toxicol.* 15, 39–52.

Esswein, E., Boeniger, M.F., Ashley, K., 2011. Handwipe Method for Removing Lead from Skin. June 2019. https://www.researchgate.net/publication/239522749_Handwipe_method_for_removing_lead_from_skin.

Finizio, A., Mackay, D., Bidleman, T., Harner, T., 1997. Octanol-air partition coefficient as a predictor of partitioning of semi-volatile organic chemicals to aerosols. *Atmos. Environ.* 31, 2289–2296.

Frombach, J., Unbehauen, M., Kurniasih, I.N., Schumacher, F., Volz, P., Hadam, S., Rancan, F., Blume Peytavi, U., Kleuser, B., Haag, R., Alexiev, U., Vogt, A., 2019. Core-multishell nanocarriers enhance drug penetration and reach keratinocytes and antigen-presenting cells in intact human skin. *J. Contr. Release* 299, 138–148.

Gaga, E.O., Ari, A., 2011. Gas-particle partitioning of polycyclic aromatic hydrocarbons (PAHs) in an urban traffic site in Eskisehir, Turkey. *Atmos. Res.* 99, 207–216.

Gong, M.Y., Zhang, Y.P., Weschler, C.J., 2014. Measurement of phthalates in skin wipes: Estimating exposure from dermal absorption. *Environ. Sci. Technol.* 48, 7428–7435.

Goss, K.U., Schwarzenbach, R.P., 1998. Gas/solid and gas/liquid partitioning of organic compounds: Critical evaluation of the interpretation of equilibrium constants. *Environ. Sci. Technol.* 32, 2025–2032.

Gungormus, E., Tuncel, S., Hakan Tecer, L., Sofuoğlu, S.C., 2014. Inhalation and dermal exposure to atmospheric polycyclic aromatic hydrocarbons and associated carcinogenic risks in a relatively small city. *Ecotoxicol. Environ. Saf.* 108, 106–113.

Harrison, R.M., Brown, L.M., Collings, N., Harrison, R.M., Maynard, A.D., Maynard, R.L., Shi, J.P., Xi, S., Khan, A., Mark, D., Kinnersley, R., Yin, J., 2000. Measurement of number, mass and size distribution of particles in the atmosphere. *Philos. Trans. R. Soc. Lond. Ser. A-Math. Phys. Eng. Sci.* 358, 2567–2580.

Hirai, T., Yoshikawa, T., Nabeshi, H., Yoshida, T., Akase, T., Yoshioka, Y., Itoh, N., Tsutsumi, Y., 2012. Dermal absorption of amorphous nanosilica particles after topical exposure for three days. *Pharmazie* 67, 742–743.

Hu, Y.J., Bao, L.J., Huang, C.L., Li, S.M., Liu, P., Zeng, E.Y., 2018. Exposure to air particulate matter with a case study in Guangzhou: Is indoor environment a safe haven in China? *Atmos. Environ.* 191, 351–359.

Kaupp, H., McLachlan, M.S., 1999. Atmospheric particle size distributions of polychlorinated dibenzo-p-dioxins and dibenzofurans (PCDD/Fs) and polycyclic aromatic hydrocarbons (PAHs) and their implications for wet and dry deposition. *Atmos. Environ.* 33, 85–95.

Kim, K.E., Cho, D., Park, H.J., 2016. Air pollution and skin diseases: Adverse effects of airborne particulate matter on various skin diseases. *Life Sci.* 152, 126–134.

Lademann, J., Richter, H., Teichmann, A., Otberg, N., Blume Peytavi, U., Luengo, J., Weiss, B., Schaefer, U.F., Lehr, C.M., Wepf, R., Sterry, W., 2007. Nanoparticles—An efficient carrier for drug delivery into the hair follicles. *Eur. J. Pharm. Biopharm.* 66, 159–164.

Lademann, J., Schaefer, H., Otberg, N., Teichmann, A., Blume Peytavi, U., Sterry, W., 2004. Penetration of microparticles into human skin. *Hautarzt* 55, 1117–1119.

Lao, J.Y., Bao, L.J., Zeng, E.Y., 2018. Correction: Importance of dermal absorption of polycyclic aromatic hydrocarbons derived from barbecue fumes. *Environ. Sci. Technol.* 52, 11439–11440.

Lao, J.Y., Wu, C.C., Bao, L.J., Liu, L.Y., Shi, L., Zeng, E.Y., 2018b. Size distribution and clothing-air partitioning of polycyclic aromatic hydrocarbons generated by barbecue. *Sci. Total Environ.* 639, 1283–1289.

Lao, J.Y., Xie, S.Y., Wu, C.C., Bao, L.J., Tao, S., Zeng, E.Y., 2018c. Importance of dermal absorption of polycyclic aromatic hydrocarbons derived from barbecue fumes. *Environ. Sci. Technol.* 52, 8330–8338.

Lin, J.J., Noll, K.E., Holsen, T.M., 1994. Dry deposition velocities as a function of particle size in the ambient atmosphere. *Aerosol Sci. Technol.* 20, 239–252.

Liu, X., Shen, B.D., Shen, C.Y., Zhong, R.N., Wang, X.H., Yuan, H.L., 2018. Nanoparticle-loaded gels for topical delivery of nitrofurazone: Effect of particle size on skin permeation and retention. *J. Drug Deliv. Sci. Technol.* 45, 367–372.

Liu, Y., Gao, Y., Yu, N., Zhang, C.K., Wang, S.Y., Ma, L.M., Zhao, J.F., Lohmann, R., 2015. Particulate matter, gaseous and particulate polycyclic aromatic hydrocarbons (PAHs) in an urban traffic tunnel of China: Emission from on-road vehicles and gas-particle partitioning. *Chemosphere* 134, 52–59.

Lohmann, R., Harner, T., Thomas, G.O., Jones, K.C., 2000. A comparative study of the gas-particle partitioning of PCDD/Fs, PCBs, and PAHs. *Environ. Sci. Technol.* 34, 4943–4951.

Lohmann, R., Lammel, G., 2004. Adsorptive and absorptive contributions to the gas-particle partitioning of polycyclic aromatic hydrocarbons: State of knowledge and recommended parametrization for modeling. *Environ. Sci. Technol.* 38, 3793–3803.

Luo, P., Bao, L.J., Li, S.M., Zeng, E.Y., 2015. Size-dependent distribution and inhalation cancer risk of particle-bound polycyclic aromatic hydrocarbons at a typical e-waste recycling and an urban site. *Environ. Pollut.* 200, 10–15.

Mills, N.L., Donaldson, K., Hadoke, P.W., Boon, N.A., MacNee, W., Cassee, F.R., Sandström, T., Blomberg, A., Newby, D.E., 2008. Adverse cardiovascular effects of air pollution. *Nat. Clin. Pract. Cardiovasc. Med.* 6, 36.

Odabasi, M., Cetin, E., Sofuoğlu, A., 2006. Determination of octanol-air partition coefficients and supercooled liquid vapor pressures of PAHs as a function of temperature: Application to gas-particle partitioning in an urban atmosphere. *Atmos. Environ.* 40, 6615–6625.

Pankow, J.F., 1987. Review and comparative-analysis of the theories on partitioning between the gas and aerosol particulate phases in the atmosphere. *Atmos. Environ.* 21, 2275–2283.

Pankow, J.F., 1991. Common gamma-intercept and single compound regressions of gas particle partitioning data vs 1/T. *Atmos. Environ. Part A-General Topics* 25, 2229–2239.

Pankow, J.F., 1994. An absorption-model of gas-particle partitioning of organic-compounds in the atmosphere. *Atmos. Environ.* 28, 185–188.

Poothong, S., Padilla-Sanchez, J.A., Papadopoulou, E., Giovanoulis, G., Thomsen, C., Haug, L.S., 2019. Hand wipes: A useful tool for assessing human exposure to poly- and perfluoroalkyl substances (PFASs) through hand-to-mouth and dermal contacts. *Environ. Sci. Technol.* 53, 1985–1993.

Shen, G.F., Wang, W., Yang, Y.F., Ding, J.N., Xue, M.A., Min, Y.J., Zhu, C., Shen, H.Z., Li, W., Wang, B., Wang, R., Wang, X.L., Tao, S., Russell, A.G., 2011. Emissions of pahs from indoor crop residue burning in a typical rural stove: Emission factors, size distributions, and gas-particle partitioning. *Environ. Sci. Technol.* 45, 1206–1212.

Shi, S.S., Zhao, B., 2014. Modeled exposure assessment via inhalation and dermal pathways to airborne semivolatile organic compounds (SVOCs) in residences. *Environ. Sci. Technol.* 48, 5691–5699.

Sitaras, I.E., Bakeas, E.B., Siskos, P.A., 2004. Gas/particle partitioning of seven volatile

- polycyclic aromatic hydrocarbons in a heavy traffic urban area. *Sci. Total Environ.* 327, 249–264.
- Stapleton, H.M., Kelly, S.M., Allen, J.G., McClean, M.D., Webster, T.F., 2008. Measurement of polybrominated diphenyl ethers on hand wipes: Estimating exposure from hand-to-mouth contact. *Environ. Sci. Technol.* 42, 3329–3334.
- Stevenson, P.H., 1937. Height-weight-surface formula for the estimation of body surface area in Chinese subjects. *Chin. J. Physiol.* 12, 327–330.
- Sun, Q.H., Wang, A.X., Jin, X.M., Natanzon, A., Duquaine, D., Brook, R.D., Aguinaldo, J.G.S., Fayad, Z.A., Fuster, V., Lippmann, M., Chen, L.C., Rajagopalan, S., 2005. Long-term air pollution exposure and acceleration of atherosclerosis and vascular inflammation in an animal model. *JAMA, J. Am. Med. Assoc.* 294, 3003–3010.
- Tan, H.L., Chen, D., Peng, C.F., Liu, X.T., Wu, Y., Li, X., Du, R., Wang, B., Guo, Y., Zeng, E.Y., 2018. Novel and traditional organophosphate esters in house dust from south China: Association with hand wipes and exposure estimation. *Environ. Sci. Technol.* 52, 11017–11026.
- Tasdemir, Y., Esen, F., 2007. Dry deposition fluxes and deposition velocities of PAHs at an urban site in Turkey. *Atmos. Environ.* 41, 1288–1301.
- Vallero, D.A., 2014. *Fundamentals of Air pollution—Fifth Edition*. Elsevier, USA.
- Verdin, A., Cazier, F., Fitoussi, R., Blanchet, N., Vie, K., Courcot, D., Momas, I., Seta, N., Achard, S., 2019. An in vitro model to evaluate the impact of environmental fine particles (PM_{0.3}–2.5) on skin damage. *Toxicol. Lett.* 305, 94–102.
- Vierkoetter, A., Schikowski, T., Ranft, U., Sugiri, D., Matsui, M., Kramer, U., Krutmann, J., 2010. Airborne particle exposure and extrinsic skin aging. *J. Invest. Dermatol.* 130, 2719–2726.
- Watkins, D.J., McClean, M.D., Fraser, A.J., Weinberg, J., Stapleton, H.M., Sjodin, A., Webster, T.F., 2011. Exposure to PBDEs in the office environment: Evaluating the relationships between dust, handwipes, and serum. *Environ. Health Perspect.* 119, 1247–1252.
- WHO, 2019. *Air Pollution* (June 2019). <https://www.who.int/airpollution/household/pollutants/en/>.
- Wilson, W.E., Suh, H.H., 2012. Fine particles and coarse particles: Concentration relationships relevant to epidemiologic studies. *J. Air Waste Manag. Assoc.* 47, 1238–1249.
- Wu, C.C., Bao, L.J., Guo, Y., Li, S.M., Zeng, E.Y., 2015. Barbecue fumes: An overlooked source of health hazards in outdoor settings? *Environ. Sci. Technol.* 49, 10607–10615.
- Wu, S.P., Yang, B.Y., Wang, X.H., Yuan, C.S., Hong, H.S., 2014. Polycyclic aromatic hydrocarbons in the atmosphere of two subtropical cities in southeast China: Seasonal variation and gas/particle partitioning. *Aerosol Air Qual. Res.* 14, 1232–1246.
- Yu, C.Y., Lin, C.H., Yang, Y.H., 2010. Human body surface area database and estimation formula. *Burns* 36, 616–629.
- Yu, H., Yu, J.Z., 2012. Polycyclic aromatic hydrocarbons in urban atmosphere of Guangzhou, China: Size distribution characteristics and size-resolved gas-particle partitioning. *Atmos. Environ.* 54, 194–200.
- Zhang, K., Zhang, B.Z., Li, S.M., Zhang, L.M., Staebler, R., Zeng, E.Y., 2012. Diurnal and seasonal variability in size-dependent atmospheric deposition fluxes of polycyclic aromatic hydrocarbons in an urban center. *Atmos. Environ.* 57, 41–48.
- Zhang, L.M., Gong, S.L., Padro, J., Barrie, L., 2001. A size-segregated particle dry deposition scheme for an atmospheric aerosol module. *Atmos. Environ.* 35, 549–560.